JOURNAL OF OPTOELECTRONICS AND ADVANCED MATERIALS, Vol. 11, No. 2, February 2009, p. 197 - 203

Improvement of external extraction efficiency in light-emitting diodes using an Archimedean tiling pattern: a parametric study

JIUN-YEU CHEN[a], YI-GENG LI[b], JIA-YI YEH[c], LIEN-WEN CHEN[d], CHING-CHENG WANG[b*]
[a]*Center for General Education, Hsing Kuo University of Managementt, Tainan 709, Taiwan*
[b]*Institute of Manufacturing* Engineering*, National Cheng Kung University, Tainan 701, Taiwan*
[c]*Department of Management Information Science, Chung Hwa University of Medical Technology, Tainan 717, Taiwan*
[d]*Department of Mechanical Engineering, National Cheng Kung University, Tainan 701, Taiwan*

A theoretical discussion on the efficiency of light extraction is presented for the parameter optimization concept of the light-emitting diodes (LEDs) using a two-dimensional photonic crystal (PC). Several photonic systems of square and Archimedean lattices are investigated based on a simple design method for an efficient light output from the viewpoint of Bragg diffraction. According to the photonic band diagram, the radiation modes near the operation eigenfrequency above the light lines are used to extract light from the PC-based LED into the free space. The predicted design parameters for the optimal light extraction are qualitatively consistent with the results of three-dimensional finite-element-method simulations. The extraction efficiency could be improved by a factor of ~3 compared to that of an LED device without the PC pattern by adding an Archimedean tiling of circular pillars in the device.

(Received January 2, 2009; accepted February 23, 2009)

Keywords: Light-emitting diodes (LEDs), photonic crystals (PCs), photonic quasi-crystals (PQs), extraction enhancement

1. Introduction

Light-emitting diodes (LEDs) are promising light sources with applications in color displays, solid-state lighting, and optical communications [1-3]. One of the critical research issues in LEDs is to improve their external efficiency. It is well known that only a small fraction of photons generated in an LED device can escape, which results from the total internal reflection (TIR) at the interface of the high dielectric material and the outer medium [4]. Therefore, photons failing to radiate into the free air space are reflected back and guided laterally inside the multi-layered structure, leading to a light re-absorption. To overcome the intrinsic limitation and to extract more photons out from the device, various schemes have been explored, which include surface texturing, the use of microlenses, reshaping the light escape cone, coupling the emission to surface plasmons, and the diffraction by a two-dimensional photonic crystal (2D PC) [5-8]. Especially, high light-extraction efficiency is expected for the integration of 2D PCs, which allows the control of photonic behavior in a predictable manner.

PCs are periodic dielectric structures with a spatial scale on the order of the optical wavelength to give a particular dispersion to photons. In general, PCs can be used in two main ways in order to enhance light extraction from an LED. The first approach is the inhibition and redistribution of light emission using the significant feature of PCs, the photonic band-gaps (PBGs) [9]. However, this option generally leads to nonradiative losses and the requirement of a sufficiently large refractive index contrast to open a full band-gap [10]. The other approach is the diffraction of light due to the scattering produced by the 2D periodic array [11].The introduction of periodic patterning within the LED device causes the dispersion curves to become folded at the Brillouin zone (BZ) boundary. Thus, some of the wave-guided modes (trapped modes lying below the light line) will be easily coupled to the diffracted modes lying above the light line and escape from the device [12]. The second option is adopted here for the advantage of being compatible with present material processes and amenable to treatment in real components.

Design and optimization of the PCs are difficult due to the multi-parameter problem of a patterned texture. There are many consequences in connection with the combinations of intermixing materials, lattice symmetry, lattice constant, filling factor, shape of the scattering object, and depth of a PC layer. It is hard to confirm which one gives the most efficient PC structure in the improvement of light extraction efficiency in LEDs. To obtain high light extraction efficiency, there are some criteria based on the characteristics of PCs. For example, the BZ is close to a circle, the shape of scattering elements matches the BZ, and periodic structures with period close to the optical wavelength of the guided modes satisfy the Bragg diffraction condition. Most current implementations

of PCs in LEDs make use of square or triangular lattices. Photonic quasi-crystals (PQs) are similar to PCs but rely on a quasi-crystal arrangement of scattering elements [8, 13-16]. PQs possess high symmetry orders not achievable in nature and offer many desirable features, such as isotropic PBGs, operation in low refractive index materials, diffraction not arising from the nearest neighbor dielectric pillar interactions, eliminating artifacts due to the regularity of PCs, and flat dispersion bands. However, it is difficult to numerically establish the dispersion properties of the electromagnetic waves in most PQs, which do not have a translational symmetry but high-order rotational and line symmetries. Archimedean lattices are a category of PQs, consisting of regular convex polygons which are not necessarily identical and can fill the whole plane without gaps [15]. Only 11 kinds of Archimedean tilings with many varied geometries can be obtained, including also the familiar traditional Bravais lattices: square, triangular, and honeycomb structures. The benefits of Archimedean lattices are a higher order of local rotational symmetry than the regular lattices and the strict periodicity which allows the calculation of the dispersion relations by numerical methods. From the viewpoint of manufacture, more techniques can be used to fabricate this kind of PQs. In addition, the isotropic behaviors can be transposed to light-diffracting PQs, and the lattice constants can reach the wavelength of visible light.

The motivation for using an Archimedean lattice PC is to achieve efficient light extraction through the off-plane diffraction of the guided modes trapped within the high index layers. We present a different scheme to the optimization of light extraction efficiency in the LEDs. A kind of simple 2D PC structure constructed with a small portion of PQs is proposed for the quasi omnidirectionality of light extraction. The simulation study is also intended to compare the light extraction efficiency of the LEDs based on different kinds of periodic patterns with the pillars of circular and quadratic cross sections, and to develop the most practical design under optimized parameters. The introduction of PCs (PQs) to the improvement of extraction efficiency is discussed in detail by taking a typical organic LED structure for example. The relevance between the predictions of the plane wave expansion method (PWEM) [17] and the consequences of the three dimensional finite element method (3D FEM) calculation is demonstrated for highly efficient light-extracting structures. Our computational experiments reveal that the extraction efficiency is strongly dependent on the arrangements or arrays of the pillars and the shape of the scattering object.

2. Model design and analysis

For the theoretical study, the structures of the 2D PCs with square lattices of quadratic and circular pillars and Archimedean (4, 8^2) tilings of quadratic and circular pillars are shown in Fig. 1. All the crystals have two specific directions, Γ-X and Γ-M. The symbol (4, 8^2) is the notation to categorize the Archimedean lattices and means a tiling in which a square and two octangles gather edge-to-edge around a vertex [18]. The photonic structure of the (4, 8^2) lattice is obtained by placement of dielectric pillars at the vertices as shown in Fig. 1(b). This periodic structure can also regard as clusters of 4 atoms organized in a square Bravais lattice, i.e., a modification version of the square lattice. It indicates that Wigner-Seitz cells can be defined and all the theoretical and numerical methods already known can be applied. Photonic band diagrams can be calculated by defining periodically supercells. The primitive cell of the structure is constructed from two primitive translation vectors $\mathbf{a_1}=(1+1/\sqrt{2})a(1,1)$ and $\mathbf{a_2}=(1+1/\sqrt{2})a(-1,1)$. The positions of the basic four pillars with respect to the coordinate origin are $\mathbf{u_1}$, $\mathbf{u_2}$, $\mathbf{u_3}$ and $\mathbf{u_4}$ with $\mathbf{u_1}=a(1/2, (1/2+1/\sqrt{2}))$, $\mathbf{u_2}=a(1/2,-(1/2+1/\sqrt{2}))$, $\mathbf{u_3}=a(-1/2, -(1/2+1/\sqrt{2}))$, and $\mathbf{u_4}=a(-1/2, (1/2+1/\sqrt{2}))$, respectively. For any integers $l_{1,2}$, $\mathbf{R}=l_1\mathbf{a_1}+l_2\mathbf{a_2}$ defines the Bravais lattice with the periodic dielectric constants $\varepsilon(\mathbf{r}+\mathbf{R})=\varepsilon(\mathbf{r})$, where $\mathbf{r}$ is the position vector. Therefore, a standard PWEM can be used to calculate the band structures. The following parameters are used throughout this paper: λ is the wavelength of emission peak of active material, a is the lattice constant, s is the side of a quadratic pillar, r is the radius of a circular pillar, and d is the depth of PC (PQ) patterns. In addition, f_s (f_r) represents the ratio of side (radius) and lattice constant.

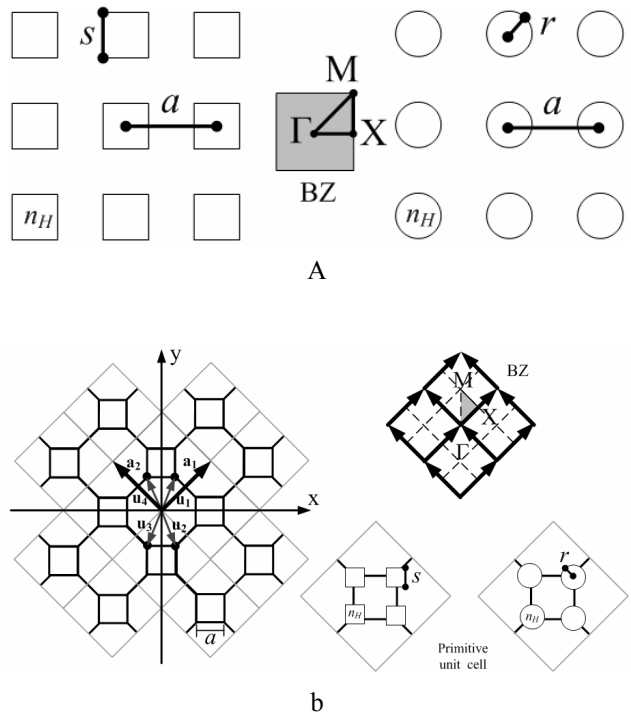

Fig. 1. 2D PCs and their associated BZs: (a) square lattices of quadratic and circular pillars; (b) (4, 8^2) Archimedean lattices of quadratic and circular pillars. These photonic structures with lattice constant a are composed of pillars with a refractive index of n_H = 1.95. The substrate refractive index is n_L = 1.48. The primitive cell in the insets of (b) included four pillars is defined by two primitive translation vectors a_1 and a_2. Four pillars surrounding the coordinate origin are at positions u_1, u_2, u_3, and u_4, respectively.

In general, the light emitted from the LED device can be classified into the following modes: the substrate mode, the waveguide mode, the radiation mode, and the surface plasmon mode [19]. From the theoretical estimation, the former two modes have the largest portion of the emitted light, which is trapped inside the device [6, 7]. In order to effectively extract the light, several possible positions in which a PC (PQ) layer or a grating can be inserted into an LED device had been previously studied [20-25]. For practical applications, the introduction of a PC (PQ) between the anode layer and the glass substrate should be the most promising, as it does not lead to a modification in the electronic properties of the device. At this interface, the PC (PQ) slab could have a strong affection on the extraction of the light confined in the waveguide and substrate modes [25]. Thus, seeking for the optimization of LED's external efficiency, it is necessary to investigate the effects of these 2D microstructures on the light emission properties of a luminescent layered material in detail. To confirm the improvement of the light extraction efficiency, the 3D FEM through the COMSOL MULTIPHYSICS^{TM} simulation software is exerted for the numerical analysis of the LED device. This method can be used to describe optical properties for considering the complexity of the model. In Fig. 2, a general schematic diagram of the modified organic LED device with a 2D PC layer [19, 23, 24] is adopted for simulations.

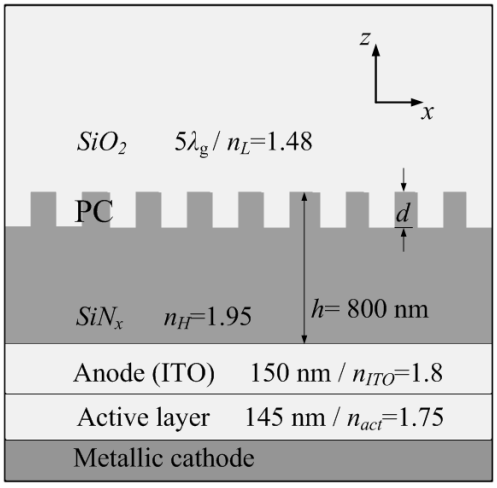

Fig. 2. Cross section view of an organic LED with SiO_2/SiN_x PC (PQ) layer. The specified refractive indices are relative to the emitting wavelength of λ_e = 530 nm.

The calculation parameters are as follows: active layer thickness $d_{act} = 145$ nm, indium-tin-oxide (ITO) anode thickness $d_{ITO} = 150$ nm, active layer refractive index $n_{act} = 1.75$, ITO refractive index $n_{ITO} = 1.8$, SiN_x refractive index $n_H = 1.95$, and SiO_2 refractive index $n_L = 1.48$. The radiation profiles of the horizontal (x and y) and the vertical (z) dipole sources are investigated by locating them at the center of the active layer. The basis elements are Lagrange-quadratic elements. The discrete model is based on a mesh limit with $\Delta x, \Delta y, \Delta z \le \lambda/(10n)$, where n is the refractive index. For the limitation of computer memory capacity, the lateral domain size of the FEM computation is restricted to a 5 ×5 square-lattice array, and the glass substrate thickness is $5\lambda_e$, where λ_e is the emission peak wavelength of the active layer (~530 nm). For simplicity, the material absorption is neglected during the calculation, and the model structure is surrounded by perfectly matched layers.

3. Numerical results and discussion

Consider 2D PC slabs made of a square lattice of SiN_x dielectric quadratic pillars with ratio $f_s = s/a = 0.38$ embedded in SiO_2 dielectric matrix. Using the PWEM, the photonic bands in transverse electric (TE, electric field lies in the 2D plane) and transverse magnetic (TM, electric field lies perpendicular to the 2D plane) modes are illustrated in Fig. 3(a). The Bloch waves to compute the eigenfrequencies are expanded by 361 plane waves. Generally, the lattice constant for PCs is set at the order of the wavelength of the relevant electromagnetic waves, $a \sim \lambda$. If the lattice constant is designed to be equal to the wavelength of the waveguide modes in the medium, the Bragg diffraction condition at the Γ point is satisfied so that the trapped light can be outcoupled [23]. In what follows, we limit ourselves to the case of normalized frequency below $a/\lambda \sim 1$. The calculated band structure of normalized frequency $\omega_n = a/\lambda$ versus wave vector $\bar{k}$ also results in the photonic density of states (DOS), which players a significant role for the understanding of the optical properties of PC-based LEDs. In the band diagram, the eigenfrequency relates to the free space wavelength of emitted light, and the wave vector relates to the azimuth angle of the emission from the active layer. The dispersion curves indicate the permitted guided or leaky modes for the emitted light. The green line indicates the light line which characterizes the TIR condition. Modes lying above the light line are leaky to radiate to free space. The intersections between the emitting center frequency and dispersion curves point out the permitted modes of emission for a PC-based LED. The use of the 2D PC (PQ) which causes the dispersion curves to become folded at the BZ boundary is to turn a waveguide mode into a radiative mode, the Bloch mode shifted above the light line. The lattice constant of the 2D pattern is designed to correlate with the wavelength of the active layer (λ_e = 530 nm) so as to induce the Bragg-diffraction effect for the emitted light. It could be expected that the extraction efficiency might be improved with the increase of DOS of the radiation mode. The right diagram in Fig. 3(a) shows the DOS of the band structure that is in connection with the radiation and waveguide modes in the PC system. It can be seen that the normalized frequency $\omega_n = 0.93$ with the maximum M^{SQ} of the DOS appear for the modes above the light line. More radiation modes appear, and the corresponding design parameters might be responsible for the most efficient light extraction. In Figs. 3(b), 3(c) and 3(d), the maxima M^{SC}, M^{AQ}, and M^{AC} can also be obtained for the square PC with $f_r = r/a = 0.35$ and the (4, 8^2) Archimedean tilings with $f_s = 0.34$ and $f_r = 0.36$, respectively.

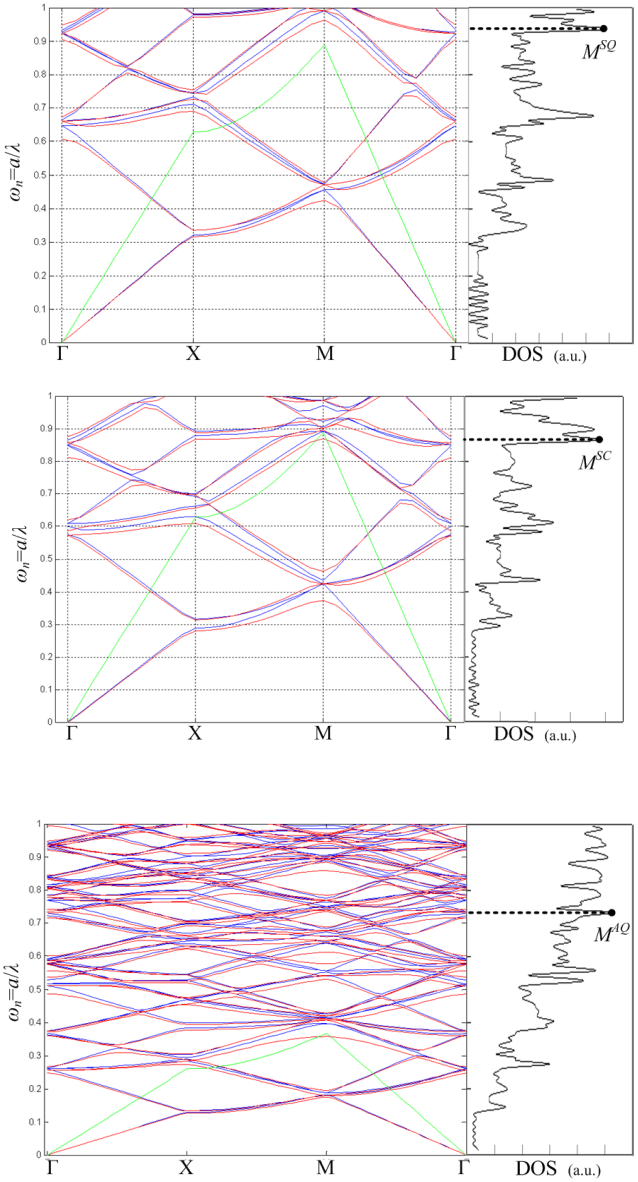

Fig. 3. Left: the dispersion relations of the 2D PCs from the lattice patterns in Fig. 1. All the calculations are made for both TE (blue lines) and TM (red lines) polarizations. Green lines represent the light line. Right: DOS calculated for the corresponding lattice textures. The ratios f_s (f_r) used for these photonic structures are (a) square: f_s = 0.38, (b) square: f_r = 0.35, (c) Archimedean: f_s = 0.34, and (d) Archimedean: f_r = 0.36. M^{SQ}, M^{SC}, M^{AQ} and M^{AC} indicate the maxima of the DOS in the dispersion diagrams, respectively. Their superscripts denote the square lattices of quadratic pillars (SQ) and circular pillars (SC) and the Archimedean lattices of quadratic pillars (AQ) and circular pillars (AC).

In addition, the effect of the variation on the side (radius) of the quadratic (circular) pillars should be evaluated to determine a moderate ratio f_s (f_r). The relationships between the maximum of the DOS and its corresponding normalized frequency from different lattices with quadratic and circular pillars are shown in Fig. 4 for different ratios of f_s (f_r). The probability in the radiative process is proportional to the DOS. For the square-lattice PC with quadratic pillars, the designed lattice constant related to the normalized frequency ω_n = 0.93 could be determined from the appropriate ratio f_s = 0.38 which corresponds to the largest value $M^{SQ}_{\max}$ among all maxima M^{SQ} in Fig. 4(a). This might be responsible for the relatively largest enhancement of the light extraction in comparison with the other ratios of f_s. For the square-lattice PC with circular pillars, the largest value $M^{SC}_{\max}$ among all maxima M^{SC} in Fig 4(b) gives the adequate ratio f_r = 0.35 and its corresponding normalized frequency ω_n = 0.86. The other normalized frequencies given by ω_n = 0.73 and 0.77 corresponding to the largest values $M^{AQ}_{\max}$ and $M^{AC}_{\max}$ at f_s = 0.34 and f_r = 0.36 can be obtained in the same way for the Archimedean PCs in Figs. 4(c) and 4(d), respectively.

In summary, the PC structure is predictable and convenient for the parameter optimization. The practices for design and optimization of the PC (PQ) texture are outlined as follows. For the selected constituent materials with different dielectric constants ($\varepsilon_H = n_H^2$, $\varepsilon_L = n_L^2$), the dispersion curves for an initial ratio $f_s = s/a$ ($f_r = r/a$) can be constructed according to the specified lattice pattern. Through the theoretical treatment of the dispersion relations, the distribution of the DOS as a function of ω_n gives a maximum DOS peak (M) for the radiation modes above the light line. By the change of the ratio f_s (f_r), the maximum M of the DOS peak can be scanned to obtain a suitable ratio f_s (f_r) which gives the largest value $M_{\max}$ and the corresponding eigenfrequency ω_n. From this eigenfrequency $\omega_n = a/\lambda$, an optimized lattice constant a could be determined to manipulate the desired emission wavelength λ. Consequently, a significant enhancement in the light extraction efficiency of the PC-based LEDs should be expected under the optimized parameters of the ratio f_s (f_r) and the eigenfrequency ω_n.

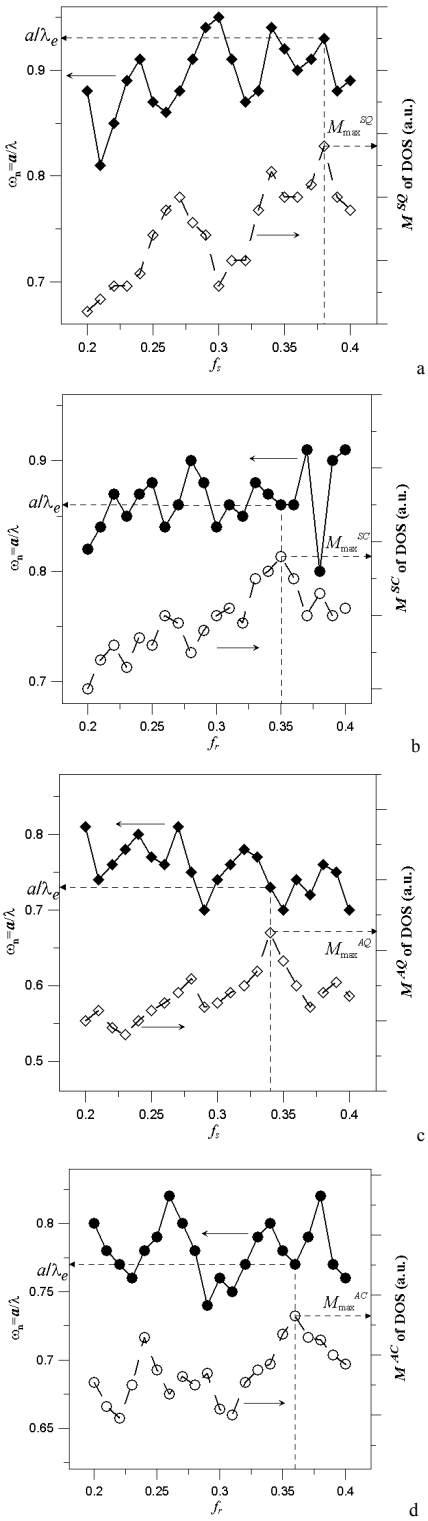

Fig. 4. The maxima of the DOS and their corresponding normalized frequencies ($\omega_n = a/\lambda$) as a function of the ratio f_s (f_r), obtained from the dispersion relations of square lattices with quadratic (a) and circular (b) pillars and (4, 8^2) lattices with quadratic (c) and circular (d) pillars. $M^{SQ}_{\max}$, $M^{SC}_{\max}$, $M^{AQ}_{\max}$, and $M^{AC}_{\max}$ represent the largest values among all maxima of the DOS for the four kinds of lattice textures, respectively.

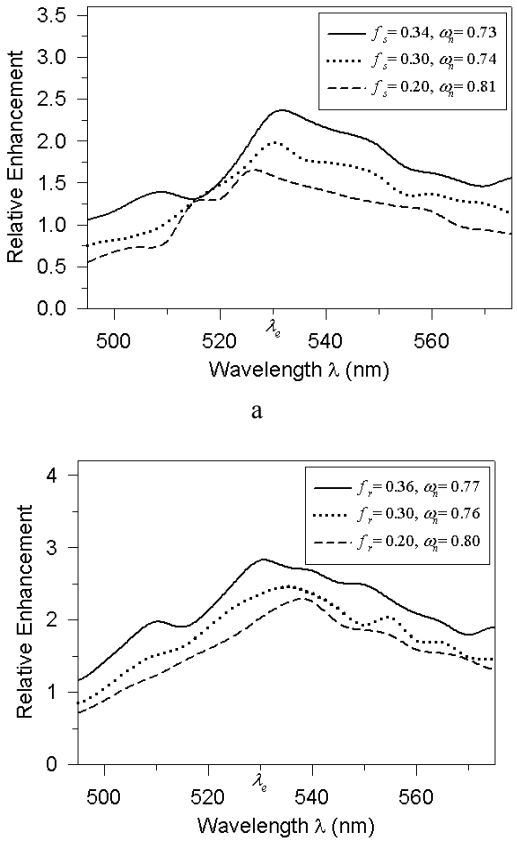

Fig. 5. Variation of the relative enhancements as a function of the emitting wavelength λ for the (4, 8^2) lattices of quadratic (a) and circular (b) pillars under the different ratios f_s (f_r) and their corresponding eigenfrequencies ω_n. The lattice constant is $a=\lambda_e\omega_n$.

Seeking for the optimization of LED's external efficiency and confirming the concepts above, the transmission properties of the PC-based organic LED are calculated by using the 3D FEM (COMSOL MULTIPHYSICS). The light output is represented by the vertical component of the Poynting vector integrated over the top surface of the organic LED device in Fig. 2. The relative enhancement is defined as the fraction of the emitted light through the top surface of the simulation model with the PC (PQ) texture to that without the PC (PQ) one. The thickness of the PC slab is taken as d = 200 nm. Under the different ratios of f_s and f_r and their corresponding eigenfrequencies ω_n in connection with the maxima M^{AQ} and M^{AC} of the DOS from Figs. 4(c) and 4(d), Fig. 5 shows the relative enhancement as a function of the emitting center wavelength λ for the Archimedean tilings of quadratic and circular pillars. The simulation results for theoretical verification are to examine the improvement of LED's relative extraction efficiency based on the concepts of the most effective PC (PQ) design. The relative light output of the organic LED is enhanced by the introduction of the PQ, and the most effective

enhancement could be attained through the parameter optimization. At the desired emitting wavelength λ_e, over 2.3 (2.8) times of the relative enhancement is observed for the optimized Archimedean tiling of quadratic (circular) pillars with the proper ratio of f_s = 0.34 (f_r = 0.36). The maximum peaks appear as a result of the multiple diffraction effects of the PQ structure.

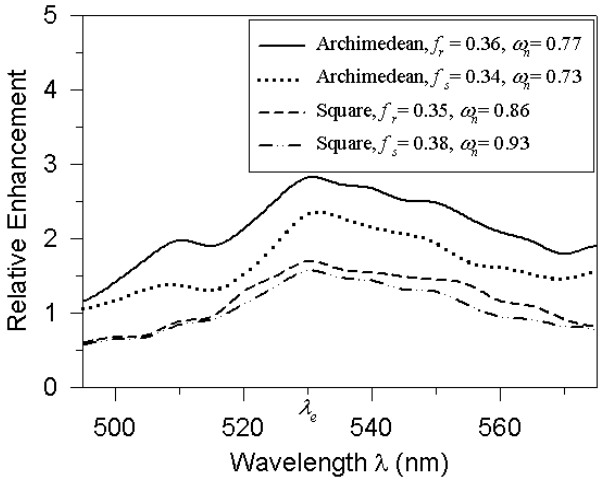

Fig. 6. Relative enhancements of the PC-based LEDs with square lattices of quadratic and circular pillars and (4, 8^2) lattices of quadratic and circular pillars are plotted as a function of the emitting wavelength of the active layer. The lattice constant is $a=\lambda_e\omega_n$.

The comparison of the relative enhancements among the four kinds of optimized PC structures (Fig. 1) embedded in the organic LED is plotted as a function of the emitting wavelength in Fig. 6. By means of 3D FEM simulations, it is shown that the amount of light extraction from the LED device with the square PC of quadratic pillars (f_s = 0.38) is 1.6 times larger than extracted from the nonpatterned device at the designed wavelength λ_e. The device containing the square PC of circular pillars (f_r = 0.35) is 1.7 times more intense than that without the PC. From Fig. 6, the following results are inferred. The lattices of circular pillars are more effective than those of quadratic pillars. The Archimedean tilings give better light extraction than the square arrangements. In Fig. 3, the results of band diagram calculations, especially the DOS in the radiation mode, are related to the extraction efficiency calculated by the 3D FEM. Additionally, the shape of the scattering elements affects the distribution of the DOS. The increase of the relative enhancement is attributed to the increase of the density of the radiation modes. The bands of the Archimedean lattices above the light lines (Fig. 3(c) and 3(d)) are much denser than those of the square lattices (Fig. 3(a) and 3(b)). It is also noted that more flat bands are around the designed normalized frequency for the Archimedean lattices, which offer the unique feature as well as the other PQs. At relatively flat bands, standing waves are formed, and the surface emission with the coupling of longitudinal and lateral modes can be achieved. This is the main reason for the higher peak enhancement in the Archimedean PCs with the adequate ratios of f_s and f_r.

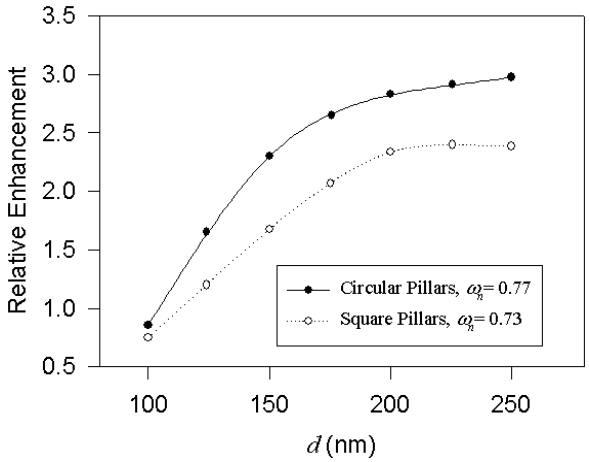

Fig. 7. Theoretical relative enhancement of light extraction efficiency versus the the PC slab thickness for (4, 8^2) lattices of quadratic and circular pillars under the specified emitting wavelength λ_e. The lattice constant is $a=\lambda_e\omega_n$.

Generally, a thicker PC layer ensures larger extraction efficiency. The PC structure as a good light extractor should result in a reasonably strong photonic interaction for high enough scattering pillars. The effect of varying the thickness d of the Archimedean PC layer is investigated on the extraction efficiency of the PC-based LED. Fig. 7 shows the enhancement ratio as a function of the PC slab thickness for the optimal PQ pattern of circular (quadratic) pillars with a ratio of f_r = 0.36 (f_s = 0.34) under the specified emitting wavelength λ_e. These results indicate that the relative enhancement increases with steep increases in the slab height up to ~150 nm and a steady upward curve above 200 nm. The maximum enhancement of the extraction efficiency is found to be by a factor of approximately 3 for the optimized PQ pattern with a thickness of d = 250 nm. However, etching very deep holes in the substrate leads to challenges for the fabrication of practical devices, so that a tradeoff should exist between the strong diffraction efficiency and some constraints.

4. Conclusions

In conclusion, we present the study of the extraction efficiency in the LED with 2D PCs including square and (4, 8^2) Archimedean lattices of quadratic pillars and those of circular pillars. As for the LED device consisting of more layers, the improvement of the extraction efficiency requires the solutions of the optimization problem involving the shape of the pillars, the dimension ratio

between the pillar and the lattice constant, the frequency of the emitting light, and the thickness of the PC slab. The numerical simulations show that the optimization concepts in the PC-based LED for both square and Archimedean lattices can increase the light extraction efficiency remarkably. This enhancement arises from the efficient diffraction of light in the normal direction by the integrated 2D PC (PQ) structure. The optimal resultant LED with (4, 8^2) lattices of circular pillars exhibits the significant improvement in light extraction, up to 3 times that of the LED without the PC integration. The predictive conditions for the optimal design from the dispersion relations through the PWEM calculations are consistent with the results of the best extraction enhancement through the 3D FEM simulations. This Archimedean PC structure can be fabricated without the complex form of the lattice pattern and can be a promising candidate for efficient LEDs.

Acknowledgements

The authors would like to thank the National Science Council (NSC) of Taiwan for financial support under contracts No. NSC 97-2221-E-432-001 and No. NSC97-2221-E-006-079-MY3.

References

[1] D. A. Steigerwald, J. C. Bhat, D. Collins, R. M. Fletcher, M. O. Holcomb, M. J. Ludowise, P. S. Martin, S. L. Rudaz, IEEE J. Selec. Topics Quantum Electron. **8**, 310 (2002).

[2] P. Bhattacharya, J. Sabarinathan, J. Topol'Ančik, S. Chakravarty, P.-C. Yu, W. Zhou, Proc. IEEE **93**, 1825 (2005).

[3] J.-M. Lourtioz, H. Benisty, V. Berger, J.-M Gérard, D. Maystre, A. Tchelnokov, Photonic Crystals: Towards Nanoscale Photonic Devices, Springer, Berlin (2005).

[4] J.-S. Kim, P. K. H. Ho, N. C. Greenham, R. H. Friend, J. Appl. Phys. **88**, 1073 (2000).

[5] K. Meerholz, D. C. Müller, Adv. Funct. Mater. **11**, 251 (2001).

[6] B. Wang, L. Ke, S.-J. Chu, J. Cryst. Growth **288**, 119 (2006).

[7] K. Ishihara, M. Fujita, I. Matsubara, T. Asano, S. Noda, H. Ohata, A. Hirasawa, H. Nakada, N. Shimoji, Appl. Phys. Lett. **90**, 111114 (2007).

[8] A. David, T. Fujii, E. Matioli, R. Sharma, S. Nakamura, S. P. DenBaars, C. Weisbuch, Appl. Phys. Lett. **88**, 073510 (2006).

[9] M. Fujita, S. Takahashi, Y. Tanaka, T. Asano, S. Noda, Science **308**, 1296 (2005).

[10] R. K. Lee, Y. Xu, A. Yariv, J. Opt. Soc. Am. B **17**, 1438 (2000).

[11] H.-Y. Ryu, J.-K. Hwang, Y.-J. Lee, Y.-H. Lee, IEEE J. Selec. Topics Quantum Electron. **8**, 231 (2002).

[12] H. Rigneault, J.-M. Lourtioz, C. Delalande, A. Levenson, Nanophotonics, ISTE, London (2006).

[13] S. David, A. Chelnokov, J.-M. Lourtioz, IEEE J. Quantum Electron. **37**, 1427 (2001).

[14] N. Horiuchi, Y. Segawa, T. Nozokido, K. Mizuno, H. Miyazaki, Opt. Lett. **29**, 1084 (2004).

[15] K. Ueda, T. Dotera, T. Gemma, Phys. Rev. B **75**, 195122 (2007).

[16] J.-Q. Li, W.-Q. Yang, Y.-T. Zhang, Q.-J. Wang, C.-P. Huang, Y.-Y. Zhu, J. Appl. Phys. **101**, 073505 (2007).

[17] J. D. Joannopoulos , S. G. Johnson, J. N. Winn, R. D. Meade, Photonic Crystals: Molding the Flow of Light, 2nd ed., Princeton University Press, Princeton (2008).

[18] B. Grünbaum and G. C. Shephard, Tilings and Patterns, Freeman, New York (1987).

[19] Y. R. Do, Y. C. Kim, Y.-W. Song, C.-O Cho, H. Jeon, Y.-J. Lee, S.-H. Kim, Y.-H. Lee, Adv. Mater. **15**, 1214 (2003).

[20] C. Liu, V. Kamaev, and Z. V. Vardenya, Appl. Phys. Lett. **86**, 143501 (2005).

[21] J. M. Ziebarth, A. K. Saafir, S. Fan, M. D. McGehee, Adv. Funct. Mater. **14**, 451 (2004).

[22] M. Fujita, T. Ueno, K. Ishihara, T. Asano, and S. Noda, H. Ohata, T. Tsuji, H Nakada, and N. Shimoji, Appl. Phys. Lett. **85**, 5769 (2004).

[23] M. Kitamura, S. Iwamoto, Y. Arakawa, Jpn. J. Appl. Phys. **44**, 2844 (2005).

[24] Y.-J. Lee, S.-H. Kim, G.-H. Kim, Y.-H. Lee, S.-H. Cho, Y.-W. Song, Y.-C. Kim, and Y. R. Do, Opt. Express **13**, 5864 (2005).

[25] P. Bienstman, P. Vandersteegen, R. Baets, Opt. Quant. Electron. **39**, 797 (2007).

*Corresponding author: n1888112@nckualumni.org.tw